HHS Public Access

Author manuscript

J Neurochem. Author manuscript; available in PMC 2018 March 01.

Published in final edited form as:

J Neurochem. 2017 March ; 140(6): 941–954. doi:10.1111/jnc.13957.

Early Involvement of Lysosome Dysfunction in the Degeneration of Cerebral Cortical Neurons Caused by the Lipid Peroxidation Product 4-Hydroxynonenal

Shi Zhang[1], **Erez Eitan**[1], and **Mark P. Mattson**[1,2,*]

[1]Laboratory of Neurosciences, National Institute on Aging Intramural Research Program, BRC 5C214, 251 Bayview Boulevard, Baltimore, MD 21224, USA

[2]Department of Neuroscience, Johns Hopkins University School of Medicine, Baltimore, MD, 21205, USA

Abstract

Free radical–mediated oxidative damage to proteins, lipids and DNA occurs in neurons during acute brain injuries and in neurodegenerative disorders. Membrane lipid peroxidation contributes to neuronal dysfunction and death, in part by disrupting neuronal ion homeostasis and cellular bioenergetics. Emerging findings suggest that 4-hydroxynonenal (HNE), an aldehyde produced during lipid peroxidation, impairs the function of various proteins involved in neuronal homeostasis. Here we tested the hypothesis that HNE impairs the cellular system that removes damaged proteins and organelles, the autophagy – lysosome pathway in rat primary cortical neurons. We found that HNE, at a concentration that causes apoptosis over a 48 – 72 hour period, increases protein levels of LC3 II and p62 and within 1 and 4 hours of exposure, respectively; LC3 II and p62 immunoreactive puncta were observed in the cytoplasm of HNE-treated neurons at 6 hours. The extent of upregulation of p62 and LC3 II in response to HNE was not affected by co-treatment with the lysosome inhibitor bafilomycin A1, suggesting that effects of HNE on autophagy were secondary to lysosome inhibition. Indeed, we found that neurons exposed to HNE exhibit elevated pH levels, and decreased protein substrate hydrolysis and cathepsin B activity. Neurons exposed to HNE also exhibited the accumulation of K63-linked polyubiquitinated proteins, which are substrates targeted for lysosomal degradation. Moreover, we found that levels of LAMP2a and Hsc70, and numbers of LAMP2a-positive lysosomes, are decreased in neurons exposed to HNE. Our findings demonstrate that the lipid peroxidation product HNE causes early impairment of lysosomes which may contribute to the accumulation of damaged and dysfunctional proteins and organelles and consequent neuronal death. Because impaired lysosome function is increasingly recognized as an early event in the neuronal death that occurs in neurodegenerative disorders, our findings suggest a role for HNE in such lysosomal dysfunction.

Graphical Abstract

Correspondence: Mark P. Mattson, mark.mattson@nih.gov.

Conflicts of interest: The authors have no conflicts of interest to declare.

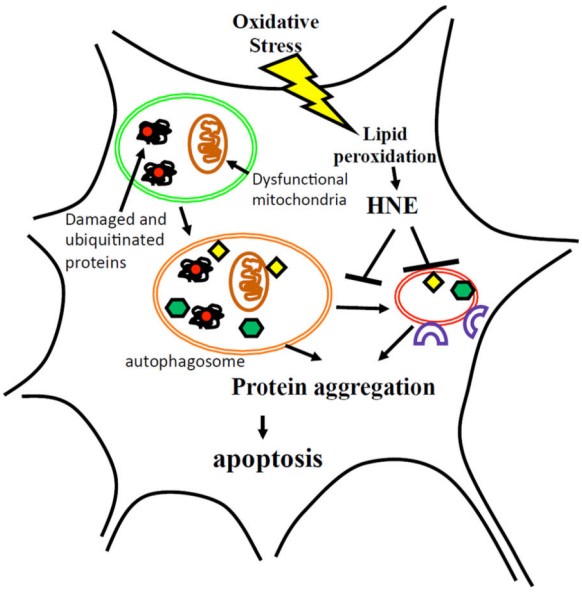

Oxidative stress, membrane lipid peroxidation and impaired lysosome function and autophagy are common features of neurodegenerative disorders. We found that the lipid peroxidation product 4-hydroxynonenal (HNE) can trigger a relatively slow form of neuronal death characterized by early inhibition of lysosome function and accumulation of autophagosomes and ubiquitinated protein aggregates.

Introduction

Aging is the major risk factor in many neurodegenerative diseases including Alzheimer's disease (AD), Parkinson's disease (PD) and amyotrophic lateral sclerosis (Mattson and Magnus, 2006; Duncan, 2011). On a per unit weight basis, the basal rate of energy consumption of the human brain is much greater than any other organ (Emerit et al., 2004). Because of their high metabolic activity, neurons generate correspondingly high levels of superoxide and hydrogen peroxide which can, in turn, generate hydroxyl radical and peroxynitrite, two free radicals that initiate membrane lipid peroxidation (Wang and Michaelis, 2010; Texel and Mattson, 2011). Neuronal membranes are rich in polyunsaturated fatty acids that are susceptible to lipid peroxidation, an autocatalytic process that generates the potentially cytotoxic aldehyde 4-hydroxynonenal (HNE). HNE is an amphipathic molecule that can covalently modify cysteine, lysine and histidine residues of proteins in many subcellular compartments, including the cytosol, mitochondria and nucleus (Uchida, 2003; Mattson, 2009). Glutathione, a tripeptide with a cysteine residue binds and thereby detoxifies HNE (Kruman et al., 1997; Perluigi et al., 2012). In the brains of AD and PD patients, and in experimental models relevant to these neurodegenerative disorders, HNE accumulates in brain cells in concentrations of 1 – 100 μM (Mark et al., 1997; Lovell et al., 1997; Markesbery and Lovell, 1998; Perluigi et al., 2012). HNE can trigger the aggregation of proteins involved in the pathogenesis of AD and PD including amyloid β-peptide (Aβ) and α-synuclein (Chen et al., 2006; Plotegher and Bubacco, 2016). In addition, HNE can cause synaptic dysfunction and neuronal death in cell culture and animal models relevant to

AD and PD (Keller et al., 1997; Kruman et al., 1997; Mark et al., 1997; Mark et al., 1997). HNE-protein adducts are detected in inclusions of vulnerable brain regions in PD (Yoritaka et al., 1996), Lewy body dementia (Dalfo et al., 2005), AD (Butterfield et al., 2001; Reed et al., 2009; Hardas et al., 2013) and Down syndrome (Di Domenico et al., 2014), and in spinal cord motor neurons in ALS patients (Pedersen et al., 1998; Kabuta et al., 2015).

Autophagy is a process in which damaged/aggregating proteins are transferred to lysosomes wherein they are degraded. Recent findings suggest that the autophagy – lysosome pathway is impaired in AD and PD (reviewed by Nixon, 2013). Neurons may be particularly prone to impaired lysosomal degradation of autophagic substrates because of their large size, high rates of metabolism and generation of reactive oxygen species, and in contrast to mitotic cells, postmitotic neurons are unable to segregate and dilute substrates during cell division. Vulnerable neurons in AD exhibit the accumulation of autophagic vesicles and autolysosomes in neuritic swellings, and inhibition of lysosome function can cause similar neuritic pathology in wild type mice and can exacerbate autophagic pathology in mouse models of AD (Nixon and Yang, 2011). Mutations in presenilin 1 that cause autosomal dominant early-onset AD impair lysosome function, apparently by compromising a normal function of presenilin 1 in promoting lysosomal acidification (Lee et al., 2010). Accumulation of markers of macroautophagy, including LC3II and p62 are increased in association with neuronal degeneration in AD (Kusisito et al., 2001). On the other hand, markers of chaperone-mediated autophagy (CMA) including LAMP2a and Hsc70, which involves targeting of ubiquitinated proteins to the lysosomes, are reduced in affected neurons in PD (Alvarez-Erviti et al., 2010).

Emerging evidence suggests that HNE can alter the autophagy – lysosome pathway. Tumor cells and smooth muscle cells exposed to HNE exhibit increased levels of LC3 II in differentiated SH-SY5Y neuroblastoma cells and aortic smooth muscle cells (Hill et al. 2008; Dodson et al. 2013). The removal of HNE-protein adducts is accelerated by the autophagy inducer, rapamycin, and decreased by the autophagy inhibitor 3-methyladenine (3-MA) (Hill et al., 2008). HNE-modified photoreceptor outer segments inhibit autophagy and enhance lipofuscinogenesis in human retinal pigment epithelium, which is associated with inhibition of the lysosomal enzymes cathepsin B and cathepsin L (Krohne et al.; 2010, Krohne et al., 2010). However, very little is known about the role of HNE on autophagy and lysosomal function in neurons. Here we report that HNE interferes both macroautophagy and the CMA pathway by inhibiting lysosome function, which can trigger neuronal apoptosis.

Materials and Methods

Reagents

All reagents were obtained from Sigma unless otherwise specified. LysoSensor and SYBR Green PCR Master Mix were purchased from Life Technologies Inc. (Grand Island, NY). HNE and bafilomycin A1 (Baf) was from Cayman Chemical Company (Ann Arbor, MI). Rapamycin and wortmannin were purchased from Sigma Chemical Company (St. Louis, MO). DQ-BSA was from Thermo Fisher Scientific. Anti-HNE antibody was from Alpha Diagnostic (San Antonio, TX; catalog #HNE13-M). Cathepsin B and cathepsin D activity

assay kits, anti-SQSTM1/p62, anti-LAMP2a (catalog #ab18528) and anti- cathepsin B (catalog #ab58802) antibodies were from Abcam (Cambridge, MA). Anti-cleaved caspase-3 (catalog #9661)) and anti-cathepsin D (catalog # 2284) antibodies were from Cell Signaling Technology (Danvers, MA). Anti-LC3 (catalog #NB100-2220), and Anti-Hsc70 (catalog #NB120-2788) antibodies were from Novus Biologicals (Littleton, CO). Anti mono- and polyubiquitinylated conjugated antibody was from Enzo Life Sciences (Farmingdale, NY; catalog #PW8810). Anti K48-linked and K63-linked polyubiquitin antibodies (catalog number 05-1307 and 05-1308, respectively) were from EMD Millipore (Billerica, MA). MTS assay kit was from Promega Life Sciences (Madison, WI). LDH assay kit was from Roche Diagnostics (Indianapolis, IN).

Primary neuronal culture

Cultures of primary cortical neurons were prepared from embryonic day 18 (E18) Sprague-Dawley rats (purchased from Charles River Laboratories, Raleigh, NC). All animal procedures were approved by the animal care and use committee of the National Institute on Aging Intramural Research Program, and complied with NIH guidelines. Dissociated cells were plated onto polyethyleneimine-coated plastic dishes or glass coverslips in MEM medium (Invitrogen Inc., Carlsbad, CA) supplemented with 10% Hyclone III (Thermo Fisher Scientific) at a density of 3.0×10^5 cells/cm^2 for biochemistry and 1.0×10^4 cells/cm^2 for immunocytochemistry analysis. After cells attached to the surface (4 hours), the medium was changed to Neurobasal medium containing B27 supplements (Invitrogen). Every 7 days 50% of the medium volume was removed and replaced with fresh medium. Immediately prior to experimental treatment, the culture medium was replaced with fresh Neurobasal medium. HNE and bafilomycin were prepared as 2000× stocks in ethanol and dimethylsulfoxide, respectively. Control cultures were exposed to ethanol and/or dimethylsulfoxide in the same amounts as the cultures exposed to HNE and/or bafilomycin.

Cell viability assays

The MTS assay (Promega Corporation, Madison, WI) and LDH assay (Roche Life Science, Indianapolis, IN) were performed according to the manufacturer's instructions. Neurons were grown in 96-well plates at a density of 10,000 cells/well for 7 days. Different concentrations of HNE were then added to the culture medium for indicated hours. The culture medium was removed for the LDH assay and cells were left in wells for the MTS assay. The absorbance (optical density) value was read at a wavelength of 492 nm with a microplate reader (Biotek, Winooski, VT).

Cell fractionation and immunoblot analysis

For extraction of protein for immunobloting of LC3, p62, β-actin, LAMP2a, Hsc70, CathepsinB and D, the neurons were harvested, washed twice with ice-cold PBS, and lysed with RIPA lysis buffer (50 mM Tris, pH 7.4, 150 mM NaCl, 0.1% SDS, 1% NP-40, 2 mM EDTA, 1 mM DTT, 1 mM PMSF, 200 μM Na_3VO_4, 50 mM NaF and protease inhibitors (Roche)) on ice for 20 min, and centrifuged at 15,600 × g for 15 minutes. For extraction of protein for immunobloting of HNE and ubiquitin-modified proteins, the method was adopted from Choo and Zhang (2009). Neurons were lysed in 2% SDS lysis buffer (50 mM Tris-HCl, pH 7.6, 1.0% Triton X-100, 2% SDS, 10 μg/ml aprotinin, 5 mM NaF, 1 mM DTT, 1

mM PMSF, 1 mM Na_3VO_4, and protease inhibitors (Roche)), boiled at 100°C for 10 minutes, and then centrifuged at 20,000 × g for 15 minutes. The protein concentration of the supernatant was determined using a BCA protein assay kit (Thermo Fisher Scientific). Samples were heated to 70°C in NuPAGE LDS sample buffer (Invitrogen) and loaded onto NuPAGE Bis-Tris gels (Invitrogen) for protein separation. Following electrophoresis, proteins were transferred from the gel to a nitrocellulose sheet by electrophoresis and the sheet was stained with Ponceau S solution (Sigma) to briefly assess the efficiency of transfer. Then the sheet was washed with deionized-water and incubated overnight at 4°C with a primary antibody which included: anti-actin (Sigma, Saint Louis, MO; A2066), anti-HNE (Alpha Diagnostic International, San Antonio, TX; HNE13-M), anti-LC3b (Novus Biologicals, Littleton, CO; NB100-2220), anti-SQSTM1 / p62 (Abcam, Cambridge, MA; ab56416), anti-LAMP2a (Abcam; ab18528), anti-Hsp70/Hsc70 (Novus Biologicals; NB120-2788), anti- mono- and polyubiquitinylated conjugated antibody (Enzo Life Sciences, Farmingdale, NY; BML-PW8810), anti- K48-linked and K63-linked polyubiquitin antibodies (EMD Millipore, Billerica, NY; 05-1307, 05-1308), anti-cathepsin D (Cell Signaling Technology, Danvers, MA; #2284), anti-cathepsin B (Abcam; ab58802). The sheet was then incubated in the presence of HRP-conjugated secondary antibodies (Cell Signaling Technology) and the immunolabeled proteins were visualized using an enhanced chemiluminescence kit (Thermo Fisher Scientific). Analysis of immunolabeled band intensity was performed using Image J software (NIH) and values were normalized to the intensity of the actin band or Ponceau S stained bands in the same protein sample.

Immunofluorescence and confocal microscopy

Cortical neurons were grown on glass coverslips for 7 days with or without specific treatments before immunostaining. For immunostaining of cleaved caspase 3 and ubiquitin, neurons were washed in PBS twice and then fixed in PBS containing 4% paraformaldehyde for 20 min at room temperature. Cell membranes were then permeabilized by incubation in 0.2% Triton X-100 in PBS for 30 minutes. For immunostaining of LC3 and p62, neurons were washed in PBS twice and then fixed in 100% methanol for 15 min at −20 °C. After fixation, neurons were incubated in 3% bovine serum albumin in PBS for 1 hour, and then incubated with a primary antibody diluted in blocking buffer overnight at 4 °C. Primary antibodies included those against: cleaved caspase-3 (Cell Signaling Technology; # 9661), LC3 (Novus Biologicals; NB100-2220), SQSTM1/p62 (Abcam; ab56416) and mono- and poly-ubiquitinylated conjugates (Enzo Life Sciences; BML-PW8810). Alexa Fluor 488 and 568 (Invitrogen) were used as secondary antibodies. Cell nuclei were stained with Hoechst 33258 dye. Coverslips were mounted in Mountant Permafluor medium (Thermo Fisher Scientific) and visualized using a Zeiss LSM410 confocal microscope with a 40× objective lens. Images were analyzed with Image J software.

Lysosensor staining and quantification of pixel intensities

After the indicated treatments, cultured cortical neurons were incubated for 5 min in culture medium containing 1 μM LysoSensor-Green DND-189 (Invitrogen). The cells were then washed with fresh medium and observed and photographed using an Olympus IX50 fluorescence microscope with a 40× objective. The fluorescence intensity within the cell

body of 60 neurons per group was quantified from images using Image J software, and data were analyzed using GraphPad Prism 5 software.

DQ™ Red BSA assay

After 6 hours of treatment with test agents, neurons were incubated with 10 μg/ml of BSA-DQ for an additional 1 hours and then washed twice with fresh culture medium. The florescence intensity was measured using a plate reader with excitation at 578 nm and emission at 603 nm.

Cathepsin B and D activity assays

The assays were performed according to manufacturer's instructions. After treatments, neurons were washed twice in cold PBS, then lysed in chilled cell lysis buffer. After incubation on ice for 20 minutes, the cell lysates were centrifuged at 4°C at 15,600 × g for 5 minutes to remove any insoluble materials. A 50 μl aliquot of the supernatant was added to a well of a 96-well plate; 50 μl Cell Lysis Buffer was used as a control for background fluorescence. Next, 50 μl Cathepsin Reaction Buffer was added to each well, followed by 2 μl of 10 mM Cathepsin substrate. All reagents were mixed well and incubated at 37°C for 1 hour before fluorescence was measured in a fluorescence plate reader using an excitation wavelength of 400 nm and emission at 505 nm. Relative Fluorescence Units (RFU) were normalized to the total protein concentration used in the assay.

RNA isolation, RT-PCR and real-time PCR

Total RNA was isolated with Trizol RNA isolation reagent (Invitrogen), reverse transcribed to first-strand cDNA with SuperScript® III First-Strand Synthesis System (Invitrogen). For measuring the mRNA level of *p62* and *LC3*, 20 μl reaction solutions were prepared in wells of a 96 well plate using TaqMan Fast Universal PCR Master Mix (2×) (Applied Biosystems, Cat # 4367846), cDNA template and Taqman primer probes included *Gapdh* (Rn01775763_g1), *LC3B* (Rn02132764_s1) and *p62* (Rn00709977_m1). Quantitative polymerase chain reaction (Q-PCR) was carried out with StepOnePlus Real-Time PCR System. For measuring the mRNA level of LAMP2a and Hsc70, cDNA templates were amplified with SYBR Green PCR Master Mix (Invitrogen). The primers were (5' to 3'): rat-*Hsc70* forward: CAGAATCCCCAAGATCCAGA; rat-*Hsc70* reverse: GTGACATCCAAGAGCAGCAA; rat-actin forward; AAGGACTCCTATAGTGGGTGACGA; rat-actin-reverse: ATCTTCTCCATGTCGTCCCAGTTG; rat-*Lamp2a*-forward: GTCTCAAGCGCCATCATACT; rat-*Lamp2a*-reverse: TCCAAGGAGTCTGTCTTAAGTAGC. All procedures were performed according to the manufacturer's instructions. The transcription level of each gene was normalized with respect to those of *Gapdh* or β-*actin*.

Statistics

All data are presented as mean ± SEM. Comparisons between control and treatment groups were performed by using Student's unpaired t-test or analysis of variance where appropriate. Values of $p<0.05$ were considered to be statistically significant.

Results

HNE induces relatively slow degeneration of cerebral cortical neurons

To test the effects of HNE on neurons, primary rat cortical neurons were grown for 7 days in culture before experiments were initiated. In a preliminary experiment, we found that HNE concentrations of 10 μM or greater were acutely toxic, killing the neurons within 12 hours (data not shown). Using an MTS assay, we found that exposure of neurons to 5 μM HNE resulted in slow neuronal death, with no significant change in the level of MTS reduction at 12 hours or 24 hours, but a highly significant decrease in MTS reduction levels at 48 hours (66.6 ± 3.2%) and a further decrease by 72 hours (57.7 ± 4.0%) (Figure 1A). Because a decrease in MTS reduction could result from impaired mitochondrial function without cell death, we measured levels of LDH activity in the culture medium of neurons treated with HNE or vehicle for increasing time points. LDH levels in the cultured medium were relatively low at all time points examined (5 – 10% of the total amount of LDH in the cell population. However, there was a significant doubling in the amount of LDH in the medium of neurons exposed to HNE for 24, 48 or 72 hours compared to control cultures (Figure 1A). Because it was previously reported that HNE can trigger neuronal apoptosis (Kruman et al., 1997), we performed two assays to evaluate apoptosis, namely quantifying cells with condensed and fragmented nuclear DNA (Hoechst staining), and measuring relative levels of cleaved caspase 3 immunoreactivity. With each of the latter methods we found upwards of 60% of neurons exhibiting features of apoptosis in cultures treated with HNE for 48 hours, compared to 5–10% of the neurons exhibiting these signs of apoptosis in control cultures (Fig. 1C, D and E). Given that levels of MTS reduction were maintained through 24 hours of exposure to HNE, and then dropped between the 24 and 48 hour time points (Fig. 1A), the data in Fig. 1C – E suggest that HNE primarily triggers apoptosis that occurs between 24 and 48 hours of exposure. To determine whether HNE bound to proteins in the neurons, we exposed the neurons to 5 μM HNE or 0.05% ethanol (vehicle control) for 4 hours, harvested the neurons in lysis buffer and performed immunoblot analysis on the samples using an antibody against HNE-protein adducts. As expected, there were much more HNE adducts in HNE-treated neurons, especially at higher molecular weights (Figure 1B).

Evidence that HNE causes the accumulation of autophagosomes in neurons

To investigate whether the autophagy pathway is altered in neurons exposed to HNE, cortical neurons were treated with 0.05% ethanol (Con) for 24 hours or with 5 μM HNE for 1, 2, 4, 6, or 24 hours. As a positive control, neuronal cultures were treated with 100 nM bafilomycin A1 (Baf) with or without HNE for 6 hours. Bafilomycin A1 is a vacuolar ATPase inhibitor that elevates lysosomal pH and impairs fusion of autophagosomes with lysosomes, and increases the accumulation of the autophagosome-associated proteins LC3II and p62. LC3II levels increased gradually in neurons during the first 6 hours of exposure to HNE (115.1 ± 4.1%, 124.9 ± 5.3%, 129.2 ± 5.7%, 146.3 + 5.3% at 1, 2, 4 and 6 hours, respectively), then decreased at 24 hours (129.8 ± 4.4%) (Figure 2A, B). The increase of LC3II in HNE-treated neurons at 6 hours was comparable to that of neurons exposed to 100 nM Baf alone (136.0%) or co-treated with HNE (134.4%) for 6 hours. Levels of p62 levels also increased in HNE-treated neurons during the first 6 hours of exposure and then decreased by 24 hours (Figure 2C). Baf treatment resulted in a significant elevation of p62

levels (175.5 ± 9.8%) at 6 hours, and combined treatment with HNE and Baf (169.9 ± 6.8%) resulted in an elevation of p62 levels similar to that of Baf alone (Figure 2A, C). To support the hypothesis that HNE inhibits lysosomal function we inhibited the mTOR pathway with rapamycin to stimulate autophagy. Rapamycin (100 nM) alone significantly increased levels of LC3II and p62 in the neurons, and either modestly enhanced or had no effect on HNE- and bafilomycin-induced increases in levels of LC3II and p62 (Fig. 2D, E and F).

Because levels of LC3II and p62 in neurons were greatest at the 6 hour time point, we next evaluated the subcellular distribution of LC3 and p62 in neurons at that time point. Control neurons exhibited a diffuse distribution of LC3 and p62 with a few puncta in the cell body (Figure 3A, upper panels). HNE-treated neurons exhibited numerous LC3 and p62 co-immunoreactive puncta in the cell body. (Figure 3A lower panels). The number of LC3 and p62 puncta was counted in 182 control-neurons and 51 HNE-treated neurons from 3 independent experiments. There were 3.3 ± 0.2 LC3 puncta per neuron in control cultures and 7.7 ± 0.7 LC3 puncta per neuron in HNE-treated neurons ($p<0.0001$) (Figure 3B). The numbers of p62 puncta were 6.6 ± 0.4 in control neurons and 16.9 ± 1.2 in HNE-treated neurons ($p<0.0001$) (Figure 3C). To determine whether the increase of LC3II and p62 protein levels in HNE-treated neurons was a result of elevated gene expression, we performed real-time PCR to measure the levels of *LC3* and *p62* mRNAs. With *Gapdh* (glyceraldehyde-3-phosphate dehydrogenase) mRNA as an internal control, we found no decrease of *LC3* and *p62* in neurons (Figure 3D and E). Taken together, the results suggest that the increase of LC3II in HNE-treated neurons was a result of an inhibition on lysosomal degradation rather than an induction of macroautophagy flux.

Evidence that HNE inhibits lysosomes involved in chaperone-mediated autophagy

Compromised lysosome function should impair chaperone-mediated autophagy (CMA). To evaluate this possibility, we measured relative levels of Hsc70 and LAMP2a, markers of CMA (Massey et al., 2006), in control and HNE-treated neurons. The levels of LAMP2a and Hsc70 protein and mRNA were measured in neurons exposed to 5 μM HNE for increasing time periods. Levels of LAMP2a protein decreased progressively beginning within 4 hours (72.5 ± 21.8%) and continuing through 8 hours (55.3 ± 17.5%) and 24 hours (40.2 ± 26.8%) in neurons exposed to HNE (Figure 4A, B). Hsc70 protein levels were significantly reduced within 1 hour of exposure to HNE and remained reduced through 24 hours (87.9 ± 3.7%, 79.8 ± 5.8%, 82.9 ± 3.4%, 84.8 ± 5.3% and 74.9 ± 10.2% at 1, 2, 4, 8 and 24 hours, respectively) (Figure 4A, C). Levels of *Lamp2a* mRNA and *Hsc70* mRNA were not significantly affected by HNE treatment, although there was a trend towards reduced *Hsc70* mRNA levels at the 8 and 24 hour time points (Figure 4D, E).

HNE causes the accumulation of polyubiquitinated proteins in neurons

Previous findings suggest that compromised lysosome function is associated with an abnormal accumulation of polyubiquitinated proteins in vulnerable neuronal populations in AD and PD (Nixon, 2013; McKinnon and Tabrizi, 2014). Impaired lysosomal function would be expected to result in the accumulation of ubiquitinated proteins in the neurons. We therefore performed ubiquitin immunostaining in neurons exposed for 6 hours to vehicle (control) or HNE. Whereas ubiquitin-containing puncta were sparse in the neurites of

control neurons, they were abundant in the neurites of HNE-treated neurons (Figure 5A). We quantified numbers of ubiquitin immunoreactive puncta in the neurites of neurons and found that ubiquitin-containing puncta were 3-fold more abundant in HNE-treated neurons (168.2 ± 11.3%) compared to control neurons (60.6 ± 6.6%) (Figure 5B; $p<0.001$). The total amount of ubiquitin, including mono- and poly-ubiquitin, was increased by approximately 30% in neurons exposed to HNE for 6 hours (Figure 5C. D). Ubiquitinated proteins can be degraded in proteasomes and by autophagy. We used antibodies specific for either K48-linked polyubiquitin (K48-Ub, which is targeted to the proteasome) or K63-linked polyubiquitin (K63-Ub, which is targeted for lysosomal degradation) to distinguish undegraded substrates for the two different systems. Increased amounts of K48-Ub proteins were detected in HNE-treated neurons at 6 hours (Figure 5E and F), and more so at 24 hours (Figure 5I and J). Increased accumulation of K63-Ub proteins was not evident at 6 hours (Figure 5G. H) but was evident at 24 hours (Figure 5K and L).

HNE inhibits lysosomal activity in neurons

As the data to this point suggested that impairment of lysosome function is an early event in HNE-induced neuronal degeneration, we performed a series of experiments in which we evaluated the effects of HNE on indicators of lysosome functionality. First, we employed the pH-sensitive lysosome-targeted probe Lysosensor green to evaluate the relative pH of lysosomes in control and HNE-treated neurons. Cortical neurons treated with 100 μM bafilomycin A1 for 24 hours exhibited a significant decrease of Lysosensor fluorescence intensity compared with control neurons, indicating an increase of the pH within the lysosomes (Figure 6A and B). A significant decrease in Lysosensor fluorescence was detected in HNE-treated neurons within 2 hours of exposure and the fluorescence was further decreased at 24 hours (Figure 6A and B). We next evaluated the ability of lysosomes to degrade substrates using the probe DQ-BSA whose fluorescence increases after being hydrolyzed in lysosomes. HNE significantly inhibited DQ-BSA degradation in lysosomes of neurons at 6 hours (29.24 ± 9.9 % of the fluorescence level in control neurons), while 100 nM Bafilomycin A1 inhibited its degradation to 29.8 ± 4.5% (Figure 6C). Cathepsins B and D are two lysosomal enzymes that hydrolyze substrates. We measured the activities of cathepsins B and D with using commercially available kits. Levels of cathepsin D activity were not significantly reduced in neurons exposed to either HNE or bafilomycin A during a 6 hour exposure period (Figure 6D). Intriguingly, the activity of cathepsin B was greatly reduced in HNE-neurons (41.8 ± 3.9% of control neurons) and in bafilomycin A-treated neurons (63.2 ± 6.4% of control neurons) (Figure 6G). To determine whether the protein levels of cathepsins were involved in the activity of cathepsins in HNE-treated neurons, we did a WB assay on cathepsin B and D at 6 hours. Protein levels of mature cathepsin D were comparable in HNE-treated neurons, but showed a trend of increase in Baf-treated neurons (Figure S1A, B). More interestingly, immunoblot analysis also showed that levels of pro-cathepsin D (which is generated in part by the activity of cathepsin B) were decreased in neurons exposed to HNE, but not in neurons exposed to bafilomycin A (Figure 6E and F). Levels of pro-cathepsin B protein were not changed in HNE-treated neurons (Figure 6H and I), indicating that the reduction of cathepsin B activity levels was not the result of decreased levels of the enzyme. Together, these findings suggest that decreased activity of cathepsin B

at an earlier time may results in decrease of active cathepsin D in neurons with longer exposure to HNE.

Finally, to determine whether alterations macroautophagy and/or CMA upstream of lysosomes play a role in neuronal degeneration in response to HNE, we treated neurons with rapamycin to stimulate autophagy, wortmannin to inhibit autophagy upstream of lysosomes, or bafilomycin A1 to inhibit lysosomes, alone or in combination with HNE. Neuronal viability was evaluated using MTS reduction and LDH release assays. We found that inducing macroautophagy with rapamycin did not rescue the neurodegeneration caused by HNE (Figure 6J and K). Treatments with bafimolycin A1 or wortmannin enhanced HNE-induced neuronal death only modestly (Figure 6J and K). These results are consistent with HNE acting primarily by inhibiting lysosome function.

Discussion

We found that a concentration of HNE within the range of concentrations present in the cerebrospinal fluid and brain tissue of AD patients (Lovell et al., 1997; Markesbery and Lovell, 1998) impairs lysosome function in cerebral cortical neurons as indicated by decreased lysosomal pH, decreased hydrolysis of a substrate (DQ-BSA) and reduced activity of cathepsin B. This adverse effect of HNE on lysosomes is associated with the accumulation of autophagosomes and polyubquitinated proteins in the neurons, which occurs within 2 – 6 hours and many hours to days before neurons die. Neurons exposed to HNE exhibited alterations in markers of macroautophagy (LC3 and p62) and CMA (LAMP2a and Hsc-70) consistent with impairment of both pathways. The accumulation of poly-ubiquitinated proteins and autophagosomes in neurons in vulnerable brain regions are prominent features of many different neurodegenerative disorders including AD and PD (Nixon, 2013; McKinnon and Tabrizi, 2014). It was previously reported that proteasomal proteins are modified by HNE in brain tissue samples from AD patients (Cecarini et al., 2007), and that exposure of cultured motor neurons to HNE impairs proteasome activity (Keller et al., 2000). This is consistent with our finding that HNE results in increased aggregation of K48-linked polyubiquitinated proteins. Our findings that HNE impairs the degradation of K63-linked polyubiquitinated proteins and lysosome function suggest a scenario in which membrane lipid peroxidation leads to impaired lysosome function and the accumulation of dysfunctional/damaged proteins in neurons.

Membrane lipid peroxidation is implicated in the pathogenesis of age-related neurodegenerative disorders, as well as in the neuronal dysfunction and death that results from acute CNS injuries such as stroke and traumatic brain injury (Keller et al., 1998; Mattson, 2009; Sultana et al., 2013). HNE-modified proteins accumulate in association with neuronal degeneration in the brains of AD and PD patients (Sayre et al., 1997; Wataya et al., 2002). Studies of experimental neuronal culture and animal models of AD have provided evidence that lipid peroxidation and HNE impair cellular ion homeostasis and mitochondrial function in neurons, thereby rendering the neurons vulnerable to excitotoxic and metabolic stress (Keller et al., 1997; Mark et al., 1997a, 1997b). HNE may also promote amyloidogenic processing of the β-amyloid precursor protein, thereby accelerating the accumulation of Aβ (Gwon et al., 2012), and can also promote aggregation of Aβ (Siegel et

al., 2007). In the case of PD, HNE is present in abnormally high amounts in the substantia nigra (Yoritaka et al., 1996). However, it is unclear if and how HNE may contribute to the intracellular accumulation of ubiquitinated, and disease-defining pathogenic proteins in AD (pTau and Aβ) and PD (α-synuclein). Our findings suggest a potential role for HNE in an early impairment of lysosome function in the pathogenic accumulation of proteotoxic protein aggregates in neurons in proteopathic neurodegenerative disorders.

Accumulation of ubiquitinated proteins in neurons subjected to oxidative stress and HNE could result from impaired function and/or overload of the proteasomal or lysosomal degradation pathways. Numerous studies have shown that oxidative stress can impair proteasome function (Shang and Taylor, 2011), and it was also reported that HNE can impair proteasome function in cultured tumor cells and isolated proteasomes (Keller et al., 2000; Ferrington et al., 2004). Our findings suggest that HNE can also impair CMA and macroautophagy in primary cerebral cortical neurons. We found that levels of LC3II increased in cortical neurons within 1 hours of exposure to HNE, and accumulation of LC3 and p62 immunoreactive puncta in the cytoplasm within 6 hours. It was previously reported that suppression of macroautophagy by genetic deletion of Atg5 or Atg7 causes neurodegeneration in mice (Hara et al., 2006; Komatsu et al., 2006). Interestingly, a brief 30 minute exposure of cultured vascular smooth muscle cells to HNE caused a robust increase of LC3II levels and cellular vacuolization, formation of pinocytic bodies, crescent-shaped phagophores and multilamellar vesicles (Hill et al., 2008). The latter study further showed that the degradation of HNE-protein adducts could be increased with rapamycin, a well-known inducer of autophagy. We also found that levels of LAMP2a and Hsc70 decreased in neurons within 4–6 hours of exposure to HNE, consistent with an impaired ability of the neurons to recruit substrates to the lysosomes. Previous studies have shown that levels of the CMA markers LAMP2Aand Hsc70, are significantly reduced in the substantia nigra pars compacta of PD patients compared to age-matched control subjects (Alvarez-Ervitie et al., 2010). It is not known whether HNE is involved in the impairment of CMA in PD.

The specific protein target(s) involved in lysosome function that are adversely affected by HNE modification remain to be determined. One possibility is that HNE impairs the function of the vacuolar ATPase in the lysosome membrane. Consistent with this, we found that adverse effects of HNE on mitochondrial function were not exacerbated by bafilomycin A, a known inhibitor of the vacuolar ATPase. HNE may also directly inhibit cathepsin B and other lysosomal cysteine proteases by covalently modifying the enzyme active site (Crabb et al., 2002; Krohne et al., 2010). Moreover, modification of some protein substrates by HNE may render them unable to be degraded because of impaired ubiquitination, the inability of autophagic pathways to recognize or process the ubiquitinated proteins, or impaired proteolysis in the lysosome (Krohne et al., 2010). In the case of neurons, data indicate that Aβ, Tau and α-synuclein can be modified on one or more residues (Mattson et al., 1997; Qahwash et al., 2007; Xiang et al., 2015). It was reported that HNE modifies and inhibits the enzymatic activities of the lysosomal enzymes cathepsins B and L in retinal pigment epithelial cells (Krohne et al., 2012). Modification of Hsc-70 by HNE can increase the sensitivity of Hsc-70 to calpain-mediated proteolysis in hippocampal cells (Sahara and Yamashima, 2010). The latter findings are particularly interesting in light of the fact that calpains are Ca^{2+}-dependent proteases, and that HNE can destabilize neuronal Ca^{2+}

regulation, resulting elevated levels of cytosolic Ca^{2+} and vulnerability of neurons to excitotoxicity, a type of neuronal damage implicated in AD, PD and other neurodegenerative disorders (Bezprozvanny and Mattson, 2008; Schulz, 2007). Altogether, the emerging evidence suggests that disturbances in cellular redox homeostasis, energy metabolism, Ca^{2+} handling and lysosome function cross-amplify each other in neurodegenerative disorders. Our findings suggest that HNE-mediated impairment of lysosomal function may contribute to such neurodegenerative cascades.

Early preclinical findings suggest a potential for targeting HNE as a neuroprotective intervention. One approach is to scavenge HNE with peptides or modified peptides to which HNE binds covalently. For example, glutathione, a tripeptide with a cysteine residue to which HNE binds, can protect neurons against damage and death induced by lipid peroxidation and HNE (Kruman et al., 1997; Mark et al., 1997a). It was also reported that a novel histidine analog that scavenges HNE can protect neurons in cell culture and animal models of ischemic stroke (Tang et al., 2007). Another approach is to facilitate clearance of potentially pathogenic proteins by stimulating autophagy with drugs such as rapamycin (Bai et al., 2015), or interventions such as intermittent fasting and exercise (Mattson, 2012). A better understanding of the events upstream of lipid peroxidation and generation of HNE, and of the mechanisms by which HNE impairs the ability of neurons to remove potentially toxic proteins, may lead to novel approaches for preventing and treating many different neurodegenerative conditions.

Supplementary Material

Refer to Web version on PubMed Central for supplementary material.

Acknowledgments

Funding: This work was supported by the Intramural Research Program of the National Institute on Aging.

Abbreviations

Aβ	amyloid β-peptide
AD	Alzheimer’s disease
CMA	chaperone-mediated autophagy
DQ-BSA	fluorescence-quenched bovine serum albumin conjugate
HNE	4-hydroxynonenal
Hsc70	constitutively active heat-shock protein 70
LAMP2	lysosome-associated membrane protein 2
LC3	microtubule-associated protein 1A/1B light chain 3
LDH	lactate dehydrogenase

MTS	3-(4,5-dimethylthiazol-2-yl)-5-(3-carboxymethoxyphenyl)-2-(4-sulfophenyl)-2H-tetrazolium
PCR	polymerase chain reaction
PD	Parkinson’s disease

References

Alvarez-Erviti L, Rodriguez-Oroz MC, Cooper JM, Caballero C, Ferrer I, Obeso JA, Schapira AH. Chaperone-mediated autophagy markers in Parkinson disease brains. Arch Neurol. 2010; 67:1464–1472. [PubMed: 20697033]

Bai X, Wey MC, Fernandez E, Hart MJ, Gelfond J, Bokov AF, Rani S, Strong R. Rapamycin improves motor function, reduces 4-hydroxynonenal adducted protein in brain, and attenuates synaptic injury in a mouse model of synucleinopathy. Pathobiol Aging Age Relat Dis. 2015; 5:28743. [PubMed: 26306821]

Bezprozvanny I, Mattson MP. Neuronal calcium mishandling and the pathogenesis of Alzheimer's disease. Trends Neurosci. 2008; 31:454–463. [PubMed: 18675468]

Butterfield DA, Howard BJ, LaFontaine MA. Brain oxidative stress in animal models of accelerated aging and the age-related neurodegenerative disorders, Alzheimer's disease and Huntington's disease. Curr Med Chem. 2001; 8:815–828. [PubMed: 11375752]

Cecarini V, Ding Q, Keller JN. Oxidative inactivation of the proteasome in Alzheimer's disease. Free Radic Res. 2007; 41:673–680. [PubMed: 17516240]

Chen K, Maley J, Yu PH. Potential inplications of endogenous aldehydes in beta-amyloid misfolding, oligomerization and fibrillogenesis. J Neurochem. 2006; 99:1413–1424. [PubMed: 17074066]

Choo YS, Zhang Z. Detection of protein ubiquitination. J. Vis. Exp. 2009; (30):e1293.

Crabb JW, O'Neil J, Miyagi M, West K, Hoff HF. Hydroxynonenal inactivates cathepsin B by forming Michael adducts with active site residues. Protein Sci. 2002; 11:831–840. [PubMed: 11910026]

Dalfo E, Portero-Otin M, Ayala V, Martinez A, Pamplona R, Ferrer I. Evidence of oxidative stress in the neocortex in incidental Lewy body disease. J Neuropathol Exp Neurol. 2005; 64:816–830. [PubMed: 16141792]

Di Domenico F, Pupo G, Tramutola A, Giorgi A, Schinina ME, Coccia R, Head E, Butterfield DA, Perluigi M. Redox proteomics analysis of HNE-modified proteins in Down syndrome brain: clues for understanding the development of Alzheimer disease. Free Radic Biol Med. 2014; 71:270–280. [PubMed: 24675226]

Dodson M, Liang Q, Johnson MS, Redmann M, Fineberg N, Darley-Usmar VM, Zhang J. Inhibition of glycolysis attenuates 4-hydroxynonenal-dependent autophagy and exacerbates apoptosis in differentiated SH-SY5Y neuroblastoma cells. Autophagy. 2013; 9:1996–2008. [PubMed: 24145463]

Duncan GW. The aging brain and neurodegenerative diseases. Clin Geriatr Med. 2011; 27:629–644. [PubMed: 22062445]

Emerit J, Edeas M, Bricaire F. Neurodegenerative diseases and oxidative stress. Biomed Pharmacother. 2004; 58:39–46. [PubMed: 14739060]

Ferrington DA, Kapphahn RJ. Catalytic site-specific inhibition of the 20S proteasome by 4-hydroxynonenal. FEBS Lett. 2004; 578:217–223. [PubMed: 15589823]

Gwon AR, Park JS, Arumugam TV, Kwon YK, Chan SL, Kim SH, Baik SH, Yang S, Yun YK, Choi Y, Kim S, Tang SC, Hyun DH, Cheng A, Dann CE 3rd, Bernier M, Lee J, Markesbery WR, Mattson MP, Jo DG. Oxidative lipid modification of nicastrin enhances amyloidogenic gamma-secretase activity in Alzheimer's disease. Aging Cell. 2012; 11:559–568. [PubMed: 22404891]

Hara T, Nakamura K, Matsui M, Yamamoto A, Nakahara Y, Suzuki-Migishima R, Yokoyama M, Mishima K, Saito I, Okano H, Mizushima N. Suppression of basal autophagy in neural cells causes neurodegenerative disease in mice. Nature. 2006; 441:885–889. [PubMed: 16625204]

Hardas SS, Sultana R, Clark AM, Beckett TL, Szweda LI, Murphy MP, Butterfield DA. Oxidative modification of lipoic acid by HNE in Alzheimer disease brain. Redox Biol. 2013; 1:80–85. [PubMed: 24024140]

Hill BG, Haberzettl P, Ahmed Y, Srivastava S, Bhatnagar A. Unsaturated lipid peroxidation-derived aldehydes activate autophagy in vascular smooth-muscle cells. Biochem J. 2008; 410:525–534. [PubMed: 18052926]

Höhn A, Jung T, Grune T. Pathophysiological importance of aggregated damaged proteins. Free Radic Biol Med. 2014; 71:70–89. [PubMed: 24632383]

Kabuta C, Kono K, Wada K, Kabuta T. 4-Hydroxynonenal induces persistent insolubilization of TDP-43 and alters its intracellular localization. Biochem Biophys Res Commun. 2015; 463:82–87. [PubMed: 25998392]

Keller JN, Pang Z, Geddes JW, Begley JG, Germeyer A, Waeg G, Mattson MP. Impairment of glucose and glutamate transport and induction of mitochondrial oxidative stress and dysfunction in synaptosomes by amyloid beta-peptide: role of the lipid peroxidation product 4-hydroxynonenal. J Neurochem. 1997; 69:273–284. [PubMed: 9202320]

Keller JN, Kindy MS, Holtsberg FW, St Clair DK, Yen HC, Germeyer A, Steiner SM, Bruce-Keller AJ, Hutchins JB, Mattson MP. Mitochondrial manganese superoxide dismutase prevents neural apoptosis and reduces ischemic brain injury: suppression of peroxynitrite production, lipid peroxidation, and mitochondrial dysfunction. J Neurosci. 1998; 18:687–697. [PubMed: 9425011]

Keller JN, Huang FF, Markesbery WR. Decreased levels of proteasome activity and proteasome expression in aging spinal cord. Neuroscience. 2000a; 98:149–156. [PubMed: 10858621]

Keller JN, Hanni KB, Markesbery WR. Possible involvement of proteasome inhibition in aging: implications for oxidative stress. Mech Ageing Dev. 2000b; 113:61–70. [PubMed: 10708250]

Klionsky DJ. Guidelines for the use and interpretation of assays for monitoring autophagy (3rd edition). Autophagy. 2016; 12:1–222. [PubMed: 26799652]

Komatsu M, Waguri S, Chiba T, Murata S, Iwata J, Tanida I, Ueno T, Koike M, Uchiyama Y, Kominami E, Tanaka K. Loss of autophagy in the central nervous system causes neurodegeneration in mice. Nature. 2006; 441:880–884. [PubMed: 16625205]

Krohne TU, Kaemmerer E, Holz FG, Kopitz J. Lipid peroxidation products reduce lysosomal protease activities in human retinal pigment epithelial cells via two different mechanisms of action. Exp Eye Res. 2010; 90:261–266. [PubMed: 19895809]

Kruman I, Bruce-Keller AJ, Bredesen D, Waeg G, Mattson MP. Evidence that 4-hydroxynonenal mediates oxidative stress-induced neuronal apoptosis. J Neurosci. 1997; 17:5089–5100. [PubMed: 9185546]

Lee MH, Hyun DH, Jenner P, Halliwell B. Effect of proteasome inhibition on cellular oxidative damage, antioxidant defences and nitric oxide production. J Neurochem. 2001; 78:32–41. [PubMed: 11432971]

Lee JH, et al. Lysosomal proteolysis and autophagy require presenilin 1 and are disrupted by Alzheimer-related PS1 mutations. Cell. 2010; 141:1146–1158. [PubMed: 20541250]

Lovell MA, Ehmann WD, Mattson MP, Markesbery WR. Elevated 4-hydroxynonenal in ventricular fluid in Alzheimer's disease. Neurobiol Aging. 1997; 18:457–461. [PubMed: 9390770]

Mark RJ, Lovell MA, Markesbery WR, Uchida K, Mattson MP. A role for 4-hydroxynonenal, an aldehydic product of lipid peroxidation, in disruption of ion homeostasis and neuronal death induced by amyloid beta-peptide. J Neurochem. 1997a; 68:255–264. [PubMed: 8978733]

Mark RJ, Pang Z, Geddes JW, Uchida K, Mattson MP. Amyloid beta-peptide impairs glucose transport in hippocampal and cortical neurons: involvement of membrane lipid peroxidation. J Neurosci. 1997b; 17:1046–1054. [PubMed: 8994059]

Markesbery WR, Lovell MA. Four-hydroxynonenal, a product of lipid peroxidation, is increased in the brain in Alzheimer's disease. Neurobiol Aging. 1998; 19:33–36. [PubMed: 9562500]

Mattson MP. Roles of the lipid peroxidation product 4-hydroxynonenal in obesity, the metabolic syndrome, and associated vascular and neurodegenerative disorders. Exp Gerontol. 2009; 44:625–633. [PubMed: 19622391]

Mattson MP. Energy intake and exercise as determinants of brain health and vulnerability to injury and disease. Cell Metab. 2012; 16:706–722. [PubMed: 23168220]

Mattson MP, Magnus T. Ageing and neuronal vulnerability. Nat Rev Neurosci. 2006; 7:278–294. [PubMed: 16552414]

Mattson MP, Fu W, Waeg G, Uchida K. 4-Hydroxynonenal, a product of lipid peroxidation, inhibits dephosphorylation of the microtubule-associated protein tau. Neuroreport. 1997; 8:2275–2281. [PubMed: 9243625]

McKinnon C, Tabrizi SJ. The ubiquitin-proteasome system in neurodegeneration. Antioxid Redox Signal. 2014; 21:2302–23021. [PubMed: 24437518]

Nixon RA, Yang DS. Autophagy failure in Alzheimer's disease—locating the primary defect. Neurobiol. Dis. 2011; 43:38–45. [PubMed: 21296668]

Nixon RA. The role of autophagy in neurodegenerative disease. Nat Med. 2013; 19:983–997. [PubMed: 23921753]

Pedersen WA, Fu W, Keller JN, Markesbery WR, Appel S, Smith RG, Kasarskis E, Mattson MP. Protein modification by the lipid peroxidation product 4-hydroxynonenal in the spinal cords of amyotrophic lateral sclerosis patients. Ann Neurol. 1998; 44:819–824. [PubMed: 9818940]

Perluigi M, Coccia R, Butterfield DA. 4-Hydroxy-2-nonenal, a reactive product of lipid peroxidation, and neurodegenerative diseases: a toxic combination illuminated by redox proteomics studies. Antioxid Redox Signal. 2012; 17:1590–1609. [PubMed: 22114878]

Plotegher N, Bubacco L. Lysines, Achilles' heel in alpha-synuclein conversion to a deadly neuronal endotoxin. Ageing Res Rev. 2016; 26:62–71. [PubMed: 26690800]

Qahwash IM, Boire A, Lanning J, Krausz T, Pytel P, Meredith SC. Site-specific effects of peptide lipidation on beta-amyloid aggregation and cytotoxicity. J Biol Chem. 2007; 282:36987–36997. [PubMed: 17693400]

Reed TT, Pierce WM, Markesbery WR, Butterfield DA. Proteomic identification of HNE-bound proteins in early Alzheimer disease: Insights into the role of lipid peroxidation in the progression of AD. Brain Res. 2009; 1274:66–76. [PubMed: 19374891]

Sahara S, Yamashima T. Calpain-mediated Hsp70.1 cleavage in hippocampal CA1 neuronal death. Biochem Biophys Res Commun. 2010; 393:806–811. [PubMed: 20171158]

Sayre LM, Zelasko DA, Harris PL, Perry G, Salomon RG, Smith MA. 4-Hydroxynonenal-derived advanced lipid peroxidation end products are increased in Alzheimer'sdisease. J Neurochem. 1997; 68:2092–2097. [PubMed: 9109537]

Schulz JB. Mechanisms of neurodegeneration in idiopathic Parkinson's disease. Parkinsonism Relat Disord. 2007; 13(Suppl 3):S306–S308. [PubMed: 18267255]

Shang F, Taylor A. Ubiquitin-proteasome pathway and cellular responses to oxidative stress. Free Radic Biol Med. 2011; 51:5–16. [PubMed: 21530648]

Siegel SJ, Bieschke J, Powers ET, Kelly JW. The oxidative stress metabolite 4-hydroxynonenal promotes Alzheimer protofibril formation. Biochemistry. 2007; 46:1503–1510. [PubMed: 17279615]

Sultana R, Perluigi M, Allan Butterfield D. Lipid peroxidation triggers neurodegeneration: a redox proteomics view into the Alzheimer disease brain. Free Radic Biol Med. 2013; 62:157–169. [PubMed: 23044265]

Tang SC, Arumugam TV, Cutler RG, Jo DG, Magnus T, Chan SL, Mughal MR, Telljohann RS, Nassar M, Ouyang X, Calderan A, Ruzza P, Guiotto A, Mattson MP. Neuroprotective actions of a histidine analogue in models of ischemic stroke. J Neurochem. 2007; 101:729–736. [PubMed: 17254011]

Texel SJ, Mattson MP. Impaired adaptive cellular responses to oxidative stress and the pathogenesis of Alzheimer's disease. Antioxid Redox Signal. 2011; 14:1519–1534. [PubMed: 20849373]

Uchida K. 4-Hydroxy-2-nonenal: a product and mediator of oxidative stress. Prog Lipid Res. 2003; 42:318–343. [PubMed: 12689622]

Wang X, Michaelis EK. Selective neuronal vulnerability to oxidative stress in the brain. Front Aging Neurosci. 2010; 2:12. [PubMed: 20552050]

Wataya T, Nunomura A, Smith MA, Siedlak SL, Harris PL, Shimohama S, Szweda LI, Kaminski MA, Avila J, Price DL, Cleveland DW, Sayre LM, Perry G. High molecular weight neurofilament proteins are physiological substrates of adduction by the lipid peroxidation product hydroxynonenal. J Biol Chem. 2002; 277:4644–4648. [PubMed: 11733539]

Xiang W, Menges S, Schlachetzki JC, Meixner H, Hoffmann AC, Schlötzer-Schrehardt U, Becker CM, Winkler J, Klucken J. Posttranslational modification and mutation of histidine 50 trigger alpha synuclein aggregation and toxicity. Mol Neurodegener. 2015; 10:8. [PubMed: 25886189]

Yoritaka A, Hattori N, Uchida K, Tanaka M, Stadtman ER, Mizuno Y. Immunohistochemical detection of 4-hydroxynonenal protein adducts in Parkinson disease. Proc Natl Acad Sci U S A. 1996; 93:2696–2701. [PubMed: 8610103]

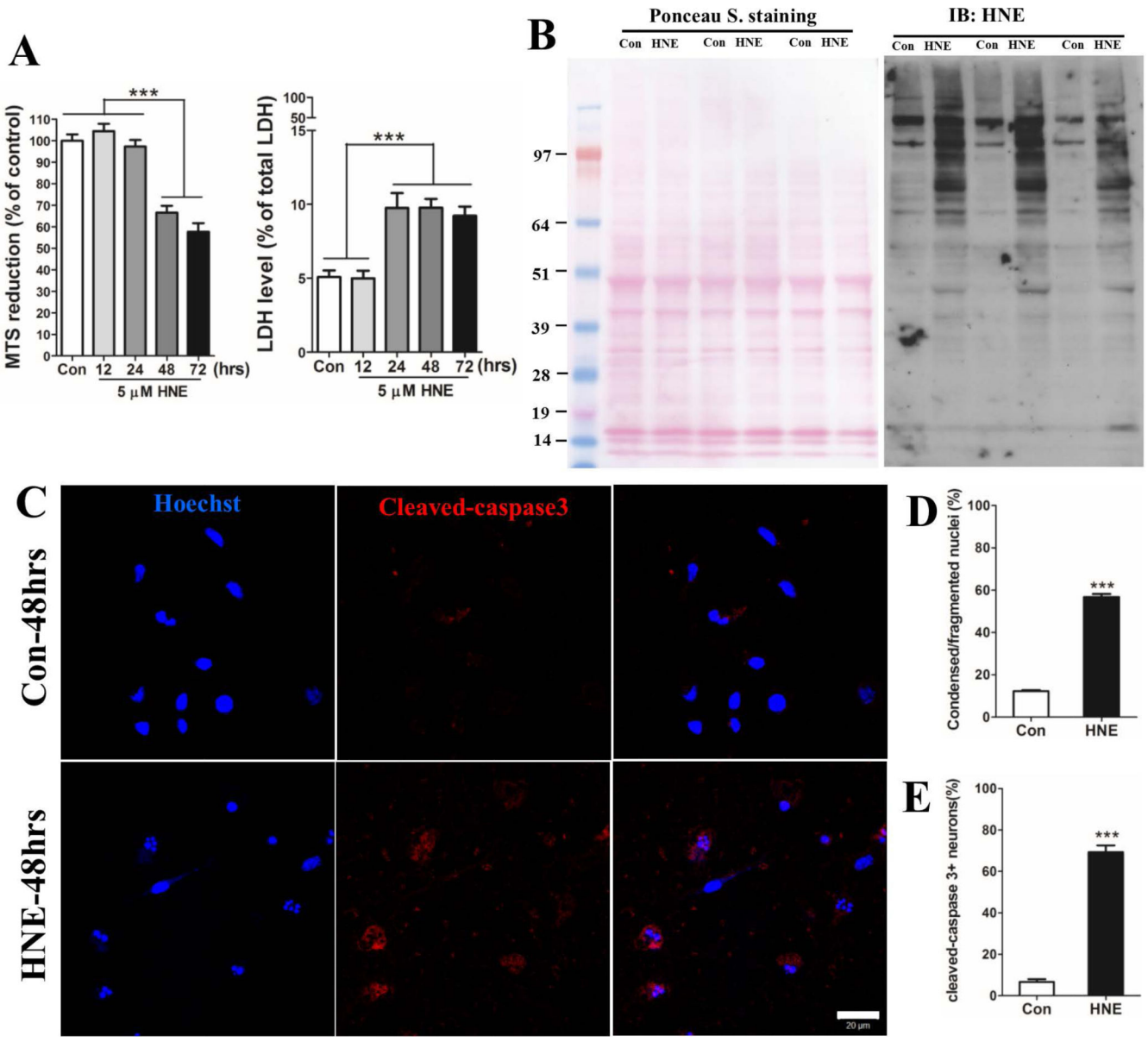

Figure 1.

HNE induces apoptosis in primary neurons. Cortical neurons were exposed to 0.05% ethanol (vehicle control; Con) or 5 μM HNE for the indicated time periods. **(A)** Levels of cellular MTS reduction (left) and LDH released into the culture medium (right). **(B)** Images showing ponceau S. staining (which stains all proteins) and HNE immunoreactive proteins on nitrocellulose from a Western blot. **(C – E)** Neurons were stained with anti-cleaved caspase-3 antibody and counterstained with Hoechst after 48 hours of treatment of with either vehicle (Con) or 5 μM HNE. Representative images are shown in panel C and results of quantitative analyses of neurons with condensed/fragmented nuclear DNA, and of neurons exhibiting cleaved caspase 3 immunoreactivity are shown in panels D and E. Results were from analyses of 310 control neurons and 355 HNE-treated neurons in three independent experiments (n = 3). ***p< 0.001 (Student's t-test). Scale bar, 20 μm.

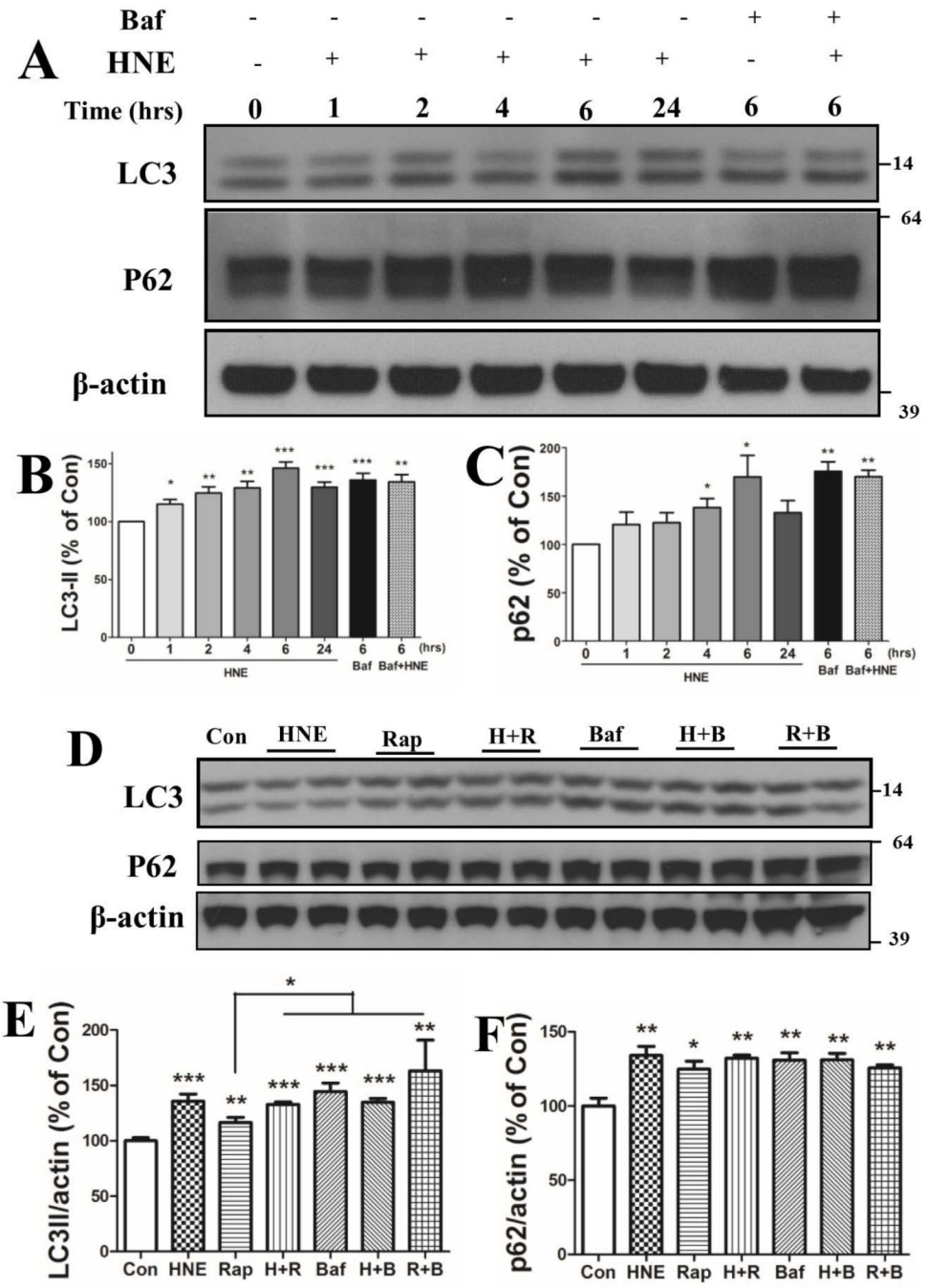

Figure 2.

HNE increases LC3 and p62 protein levels in neurons. **(A – C)** Cortical neurons were treated with 0.05% ethanol (Con) or 5 μM HNE with or without 100 μM bafilomycin A1 for the indicated time periods. Immunoblots of neuronal cell lysates were analyzed using antibodies against LC3I/II and p62, and β–actin (loading control). Representative blots are shown in panel A, and results of densitometric analysis of the LC3II, p62 and β–actin bands are shown in panels B and C. Values (mean and SEM) are from 4 independent experiments. **(D – F)** Total cellular lysates from neurons subjected to the indicated individual or combined-

treatments (5 μM HNE, 100 nM rapamycin and 100 nM bafilomycin A1) were subjected to immunoblot analysis using antibodies against LC3, p62 and β-actin. Representative blots are shown in panel D, and results of densitometric analysis of the LC3II, p62 and β–actin bands are shown in panels E and F. Values (mean and SEM) are from 4 independent experiments. *$p<0.05$, **$p<0.01$, ***$p<0.001$ compared to the control value.

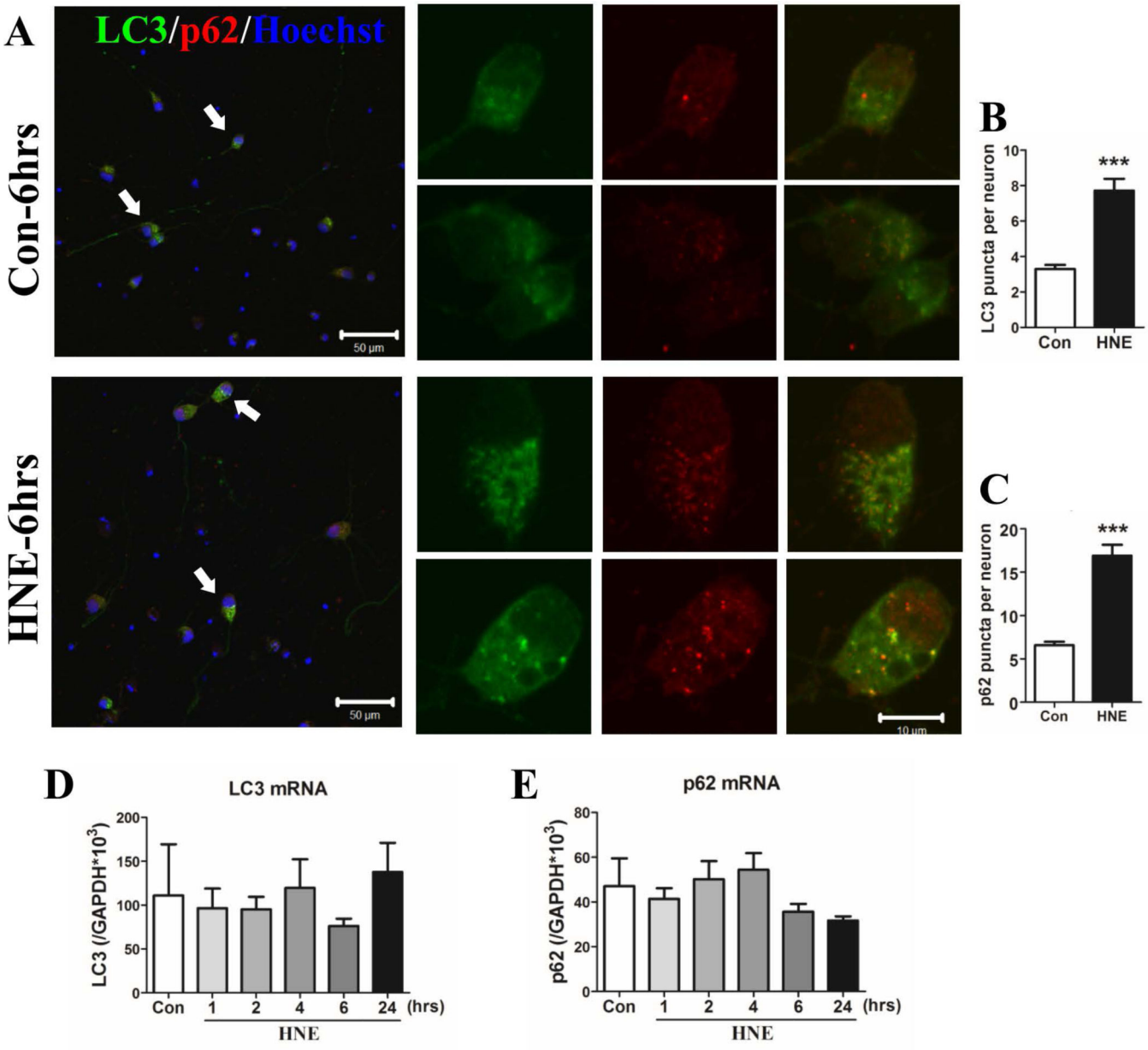

Figure 3.

HNE causes the accumulation of LC3- and p62-immunoreactive puncta in neurons without affecting *LC3* and *p62* mRNA levels. **(A)** Neurons exposed to ethanol (Con) or HNE for 6 hours were fixed with 100% cold methanol for 15 minutes at −20°C, and then co-stained with anti-LC3 (green) and anti-p62 (red) antibodies. Nuclear DNA was stained with Hoechst (blue). Images were acquired using a 40× objective with Zeiss LSM 410 confocal microscope. Representative neurons (arrows) from each group are shown in high magnification images on the right. Scale bars: 50 μm in left panels and 10 μm in right panels. **(B and C)** Numbers of LC3- and p62-positive puncta per neuron were counted. Results were from analyses of 182 control neurons and 62 HNE-treated neurons in three independent experiments (n = 3). ***p<0.001. **(D and E)** Levels of *LC3* (D) and *p62* (E)

mRNAs were quantified using real-time PCR in RNA samples from neurons treated with ethanol or HNE for the indicated time periods.

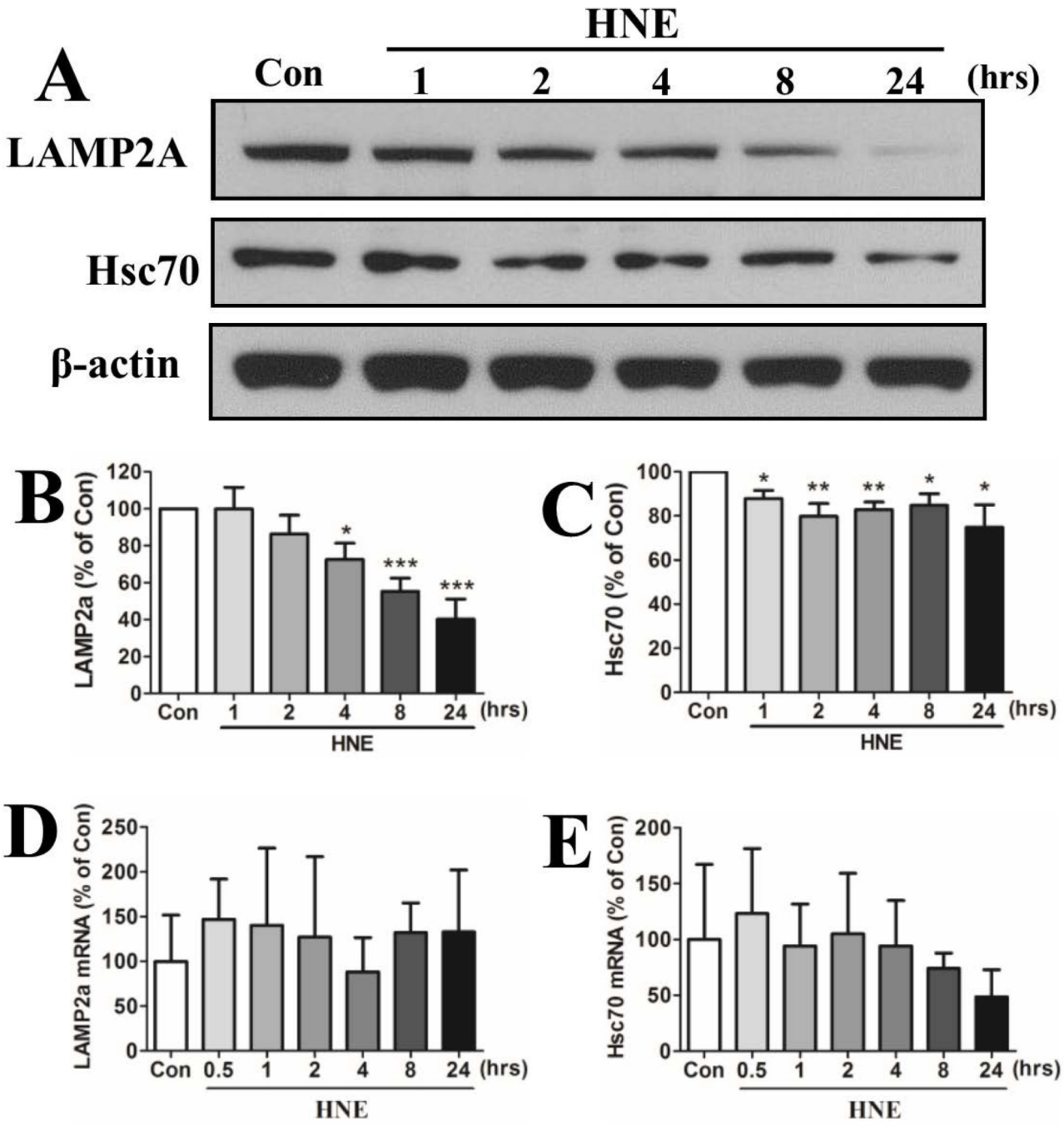

Figure 4.

Neurons exposed to HNE exhibit decreased levels of markers of chaperone-mediated autophagy. **(A)** Representative immunoblot showing relative levels of LAMP2a and Hsc70 in neurons treated with 0.05% ethanol (Con) for 24 hours or 5 μM HNE for the indicated time periods. **(B and C)** Results of densitometric analyses of immunoblots from 5 separate experiments. *p<0.05; **p<0.01; ***p<0.001 compared to the control value. **(D and E)** Levels of *Lamp2a* (D) and *Hsc70* (E) mRNAs were quantified using real-time PCR in RNA samples from neurons treated with ethanol or HNE for the indicated time periods.

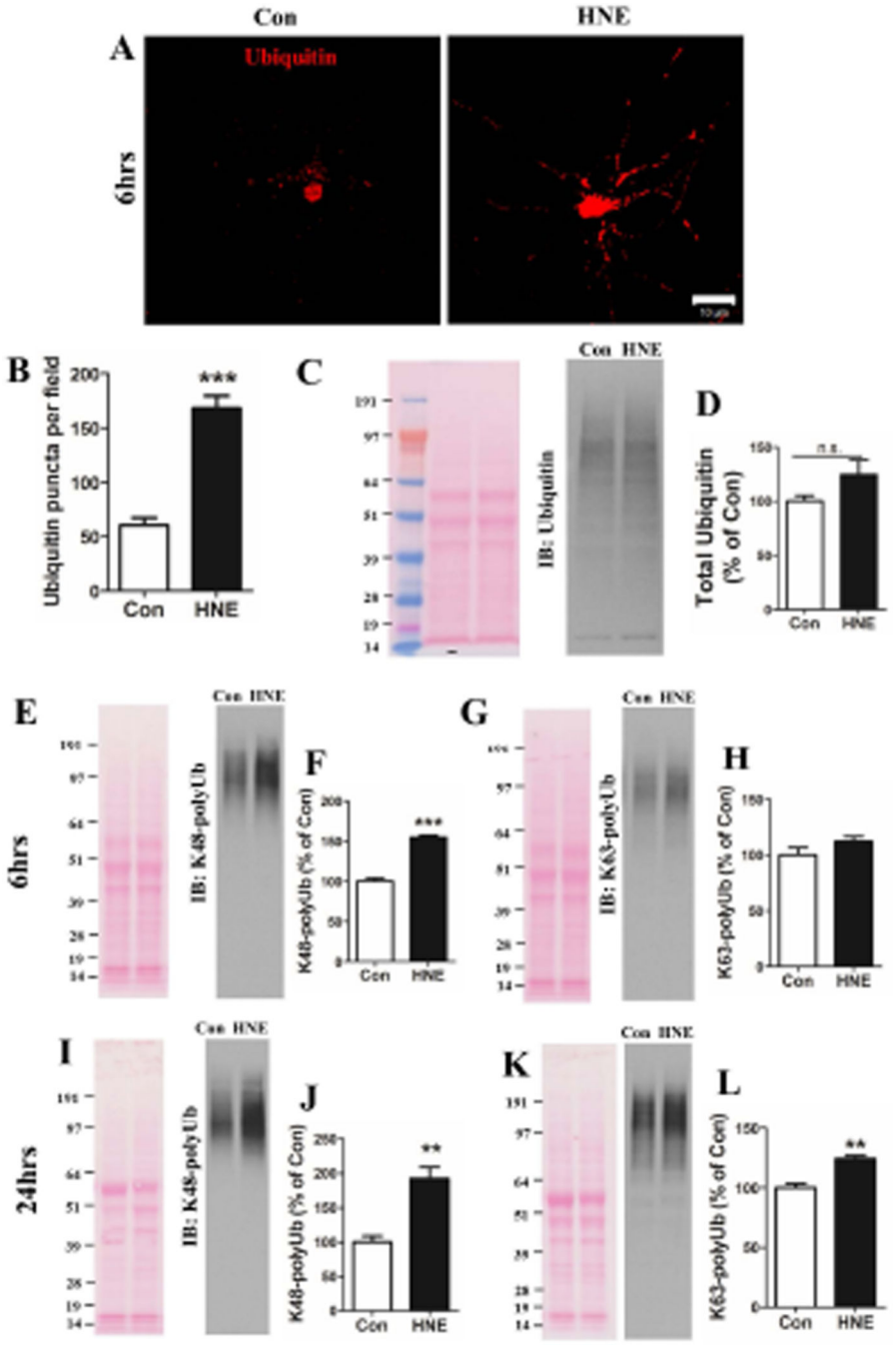

Figure 5.

Neurons exposed to HNE exhibit accumulations of polyubiquitinated proteins. **(A)** Representative images showing ubiquitinated protein immunoreactivity in neurons exposed to vehicle (Con) or 5 μM HNE for 6 hours. Scale bar, 10 μm. **(B)** Puncta of ubiquitinated protein aggregates were quantified in 22 neurons in control cultures and 30 neurons in HNE-treated neurons in 3 separate experiments. ***p<0.001. **(C, E, I J and K)** Total protein from neurons treated with ethanol or HNE for 6 hours (C, E and G) or 24 hours (I and K) were separated in 4–12% Bis-Tris gels, and the proteins were then transferred onto a

nitrocellulose membrane. Representative examples of blots stained with Ponceau S (left) and immunoreactivity with the indicated antibodies (right) are shown. **(D, F, H, J and L)** Results of densitometric analyses of immunoblots from 3 separate experiments. **p<0.01, ***p<0.001.

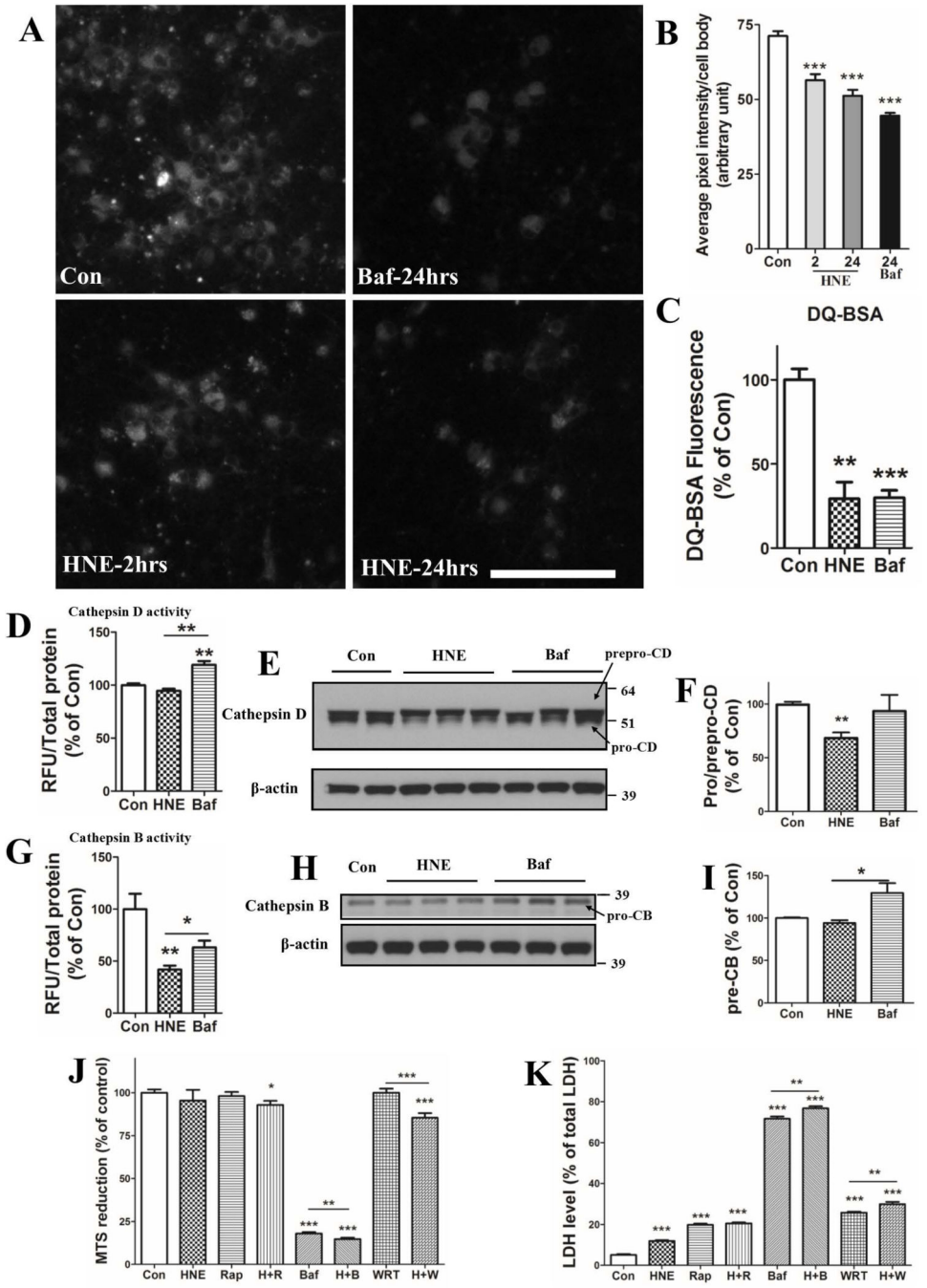

Figure 6.

HNE impairs lysosomal function. **(A and B)** Neurons were first treated with 0.05% ethanol (Con) or 100 nM bafilomycin (Baf) for 24 hours, or with 5 μM HNE for 2 and 24 hours, then incubated in the presence of LysoSensor green for 5 minutes and images of LysoSensor fluorescence were acquired. Representative images of LysoSensor fluorescence are shown in panel A and results of quantification of average fluorescence pixel intensity per cell body are shown in panel B (values are the mean and SEM of measurements made on 25 – 35 neurons in 3 separate cultures for each condition. Scale bar in panel A = 100 μm. **(C)** Neurons plated

in black-walled 96-well plates were treated for 6 hours with 0.05% ethanol (Con) 5 μM HNE or 100 nM bafilomycin A (Baf) and then subjected to the DQ-BSA protocol; fluorescence intensities were quantified using a plate reader. **(D – I)** Neurons were treated for 6 hours with 0.05% ethanol (Con) 5 μM HNE or 100 nM bafilomycin A (Baf) and then enzymatic activities (D and G) and protein levels (E, F, H and I) of cathepsins B and D were measured. Values are the mean and SEM of determinations made in 3 separate experiments. **(J and K)** Neurons were exposed to the indicated individual or combined treatments for 24 hours and neuronal viability was evaluated by MTS (J) and LDH release (K) assays. HNE, 10 μM; Rap: 100 nM rapamycin; Baf, 100 nM bafilomycin A; WRT, 5 μM wortmannin. Values are the mean and SEM of determinations made in 3 independent experiments. Differences among groups were analyzed by Student's t-test. *$p<0.05$, **$p<0.01$, ***$p<0.001$ compared to the control value or to the adjacent treatment condition as indicated.